Supplementary Information

Large Scale-up Monocrystalized 3R MoS_2 Electrocatalyst for Efficient Nitrogen Reduction Reaction

Bin Fang,[a,#] Junjie Yao,[b,#] Xiaojun Zhang,[c] Liang Ma,[c] Yaqi Ye,[b] Jiayi Tang,[b] Guifu Zou,[b] Junchang Zhang,[d,*] Lin Jiang[a,*], Yinghui Sun[b,*]

[a] *Institute of Functional Nano & Soft Materials Laboratory (FUNSOM), Jiangsu Key Laboratory for Carbon-Based Functional Materials & Devices, Soochow University, Suzhou 215123, China*

[b] *College of Energy, Soochow Institute for Energy and Materials Innovations and Key Laboratory of Advanced Carbon Materials and Wearable Energy Technologies of Jiangsu Province, Soochow University, Suzhou 215006, China*

[c] *College of Chemical Engineering, Northeast Electric Power University, Jilin, 132012, China*

[d] School of Chemistry and Chemical Engineering, Nantong University, Nantong, 226019, China

[*]Corresponding author.

E-mail address: zhangjunchang12@sina.com (J. C. Zhang); ljiang@suda.edu.cn (L. Jiang); yinghuisun@suda.edu.cn (Y. H. Sun)

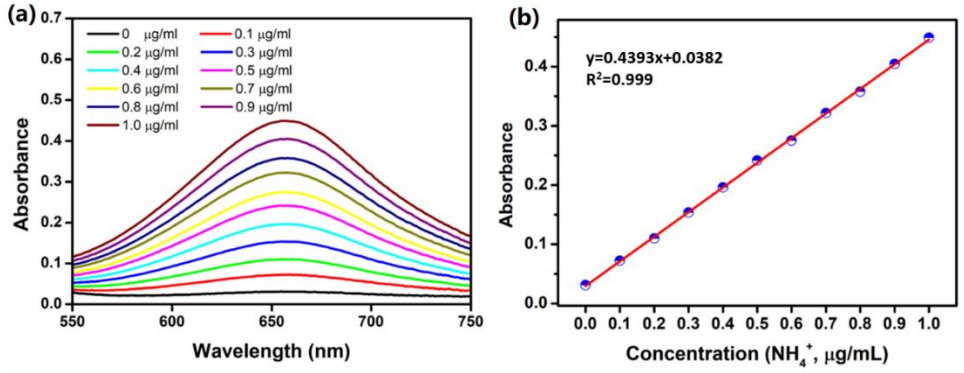

Fig. S1. (a) UV-Vis absorption spectra of various NH_4^+ concentrations after incubated for 2h at room temperature. (b) Calibration curve used for calculation of NH_3 concentrations.

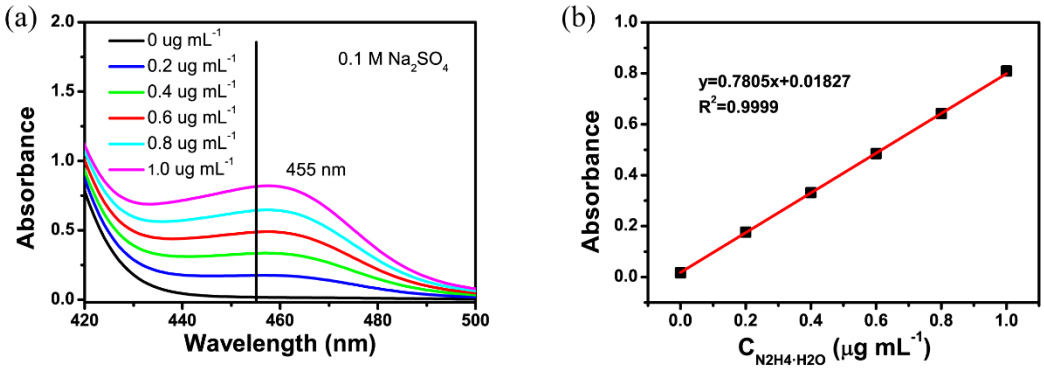

Fig. S2. (a) UV-Vis absorption spectra of various N_2H_4 concentrations after incubated for 10 min at room temperature. (b) Calibration curve used for calculation of N_2H_4 concentrations.

Fig. S3. Image of the large-scale preparation of the 3R MoS_2 in laboratory.

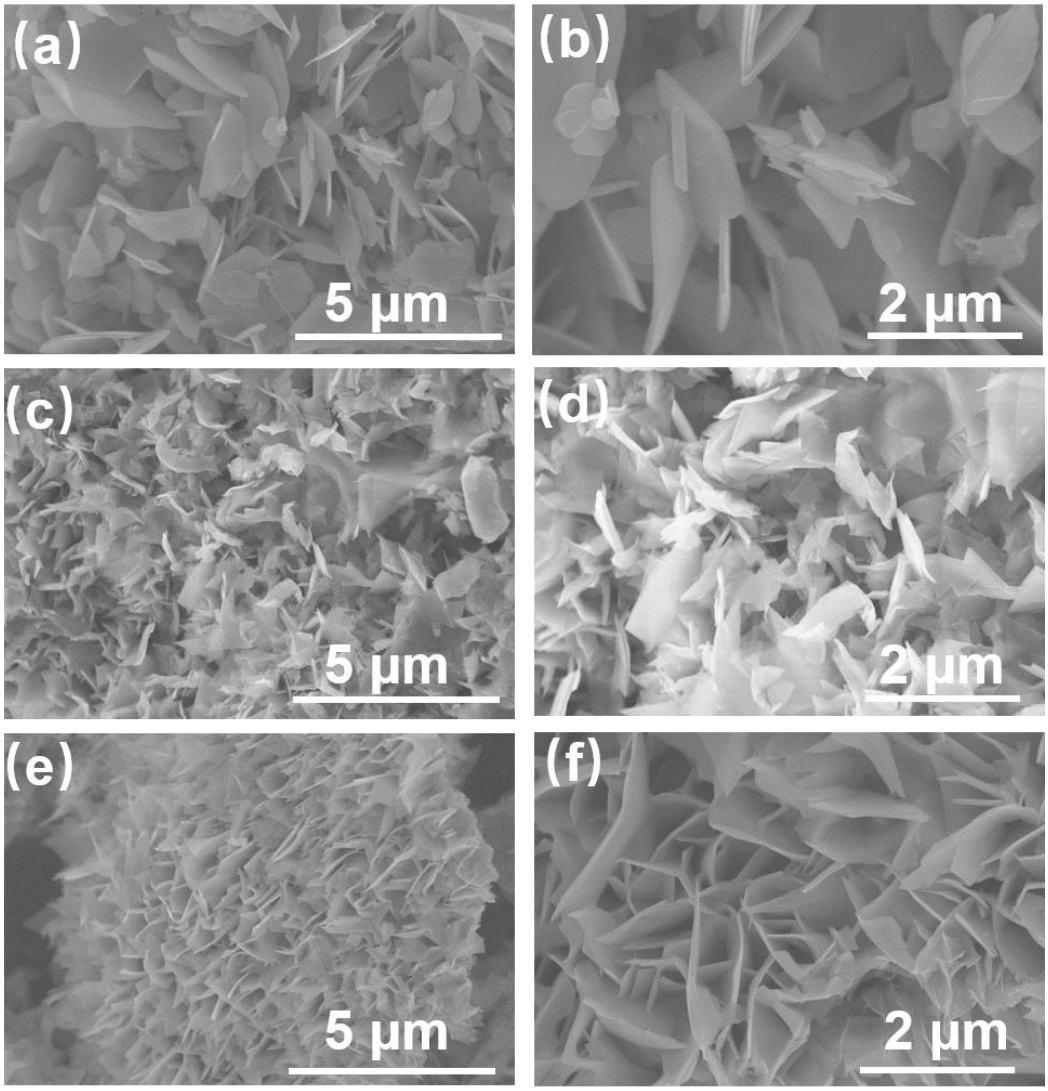

Fig. S4. SEM images of (a, b) MoS_2-600, (c, d) MoS_2-650 and (e, f) MoS_2-700.

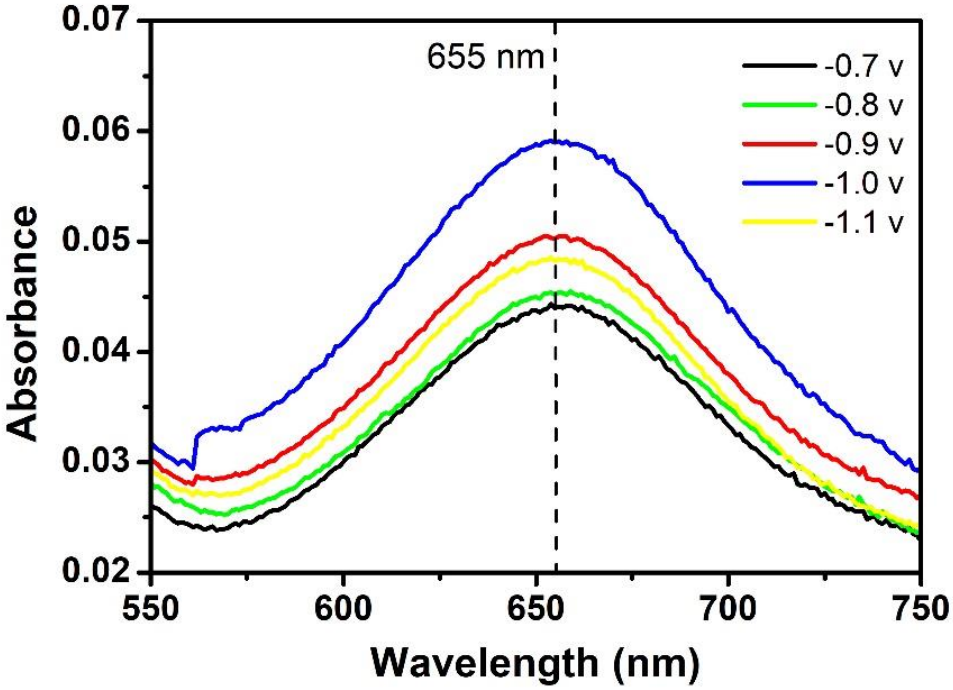

Fig. S5. UV-Vis absorption spectra of the electrolytes stained with an indophenol indicator after NRR electrolysis of MoS_2-700/CP.

Table S1. Comparison of the NRR electrocatalytic activity of 3R MoS_2 and other Mo-based catalysts at ambient condition.

Catalyst	Electrolyte	NH_3 Yield Rate	Faradic Efficiency	Reference
3R MoS_2	0.1 M Na_2SO_4	8.8 μg h^{-1} mg^{-1}_{cat}	1.9 %	This work
Mo_2C/C [a]	0.5 M Li_2SO_4	11.3 μg h^{-1} mg^{-1}_{cat}	7.8 %	[1]
MoS_2/CC [b]	0.1 M Na_2SO_4	4.94×10^{-3}μg h^{-1} cm^{-2}	1.17 %	[2]
Ru/2H-MoS_2 [c]	10 mM HCl	6.97×10^{-3}μg h^{-1} cm^{-2}	17.6 %	[3]
Fe_3Mo_3C/C [d]	0.1 M KOH	13.55 μg h^{-1} cm^{-2}	14.74 %	[4]
AuNPs@MoS_2 [e]	0.1 M Na_2SO_4	25 μg h^{-1} mg^{-1}_{cat}	9.7 %	[5]
1T-MoS_2@Ti_3C_2 [f]	0.1 M HCl	30.33 μg h^{-1} mg^{-1}_{cat}	10.94 %	[6]

[a]MoS_2 embedded in carbon nanosheets. [b]MoS_2 array grown on carbon cloth. [c]noble metal Ru-decorated 2H-MoS_2. [d]Fe_3Mo_3C and C composite. [e]1T-MoS_2 assembled on Ti_3C_2 MXene. [f]noble metal Au grown on MoS_2 nanosheets. 3R MoS_2 in this work is bare without any substrate.

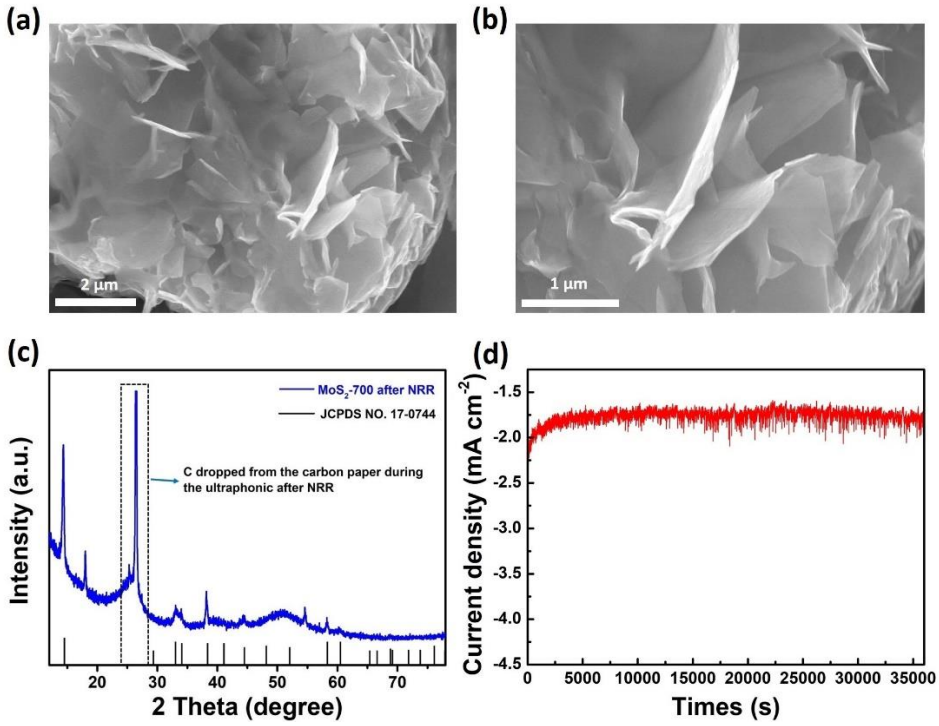

Fig. S6. SEM images (a, b) and XRD pattern (c) of MoS_2-700 after 10 h NRR electrolysis. Corresponding chronoamperometry curve tested at -1.0 V *vs.* RHE for 10 h (d).

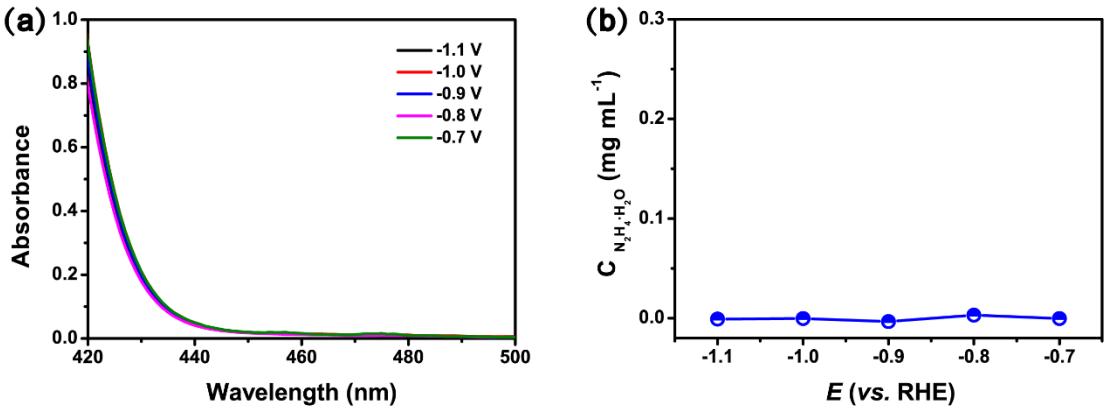

Fig. S7. UV–Vis spectra of the electrolyte estimated by the method of Watt and Chrisp after 2 h electrolysis for the NRR at different potentials under ambient conditions (a), and corresponding calculated N_2H_4 concentration (b).

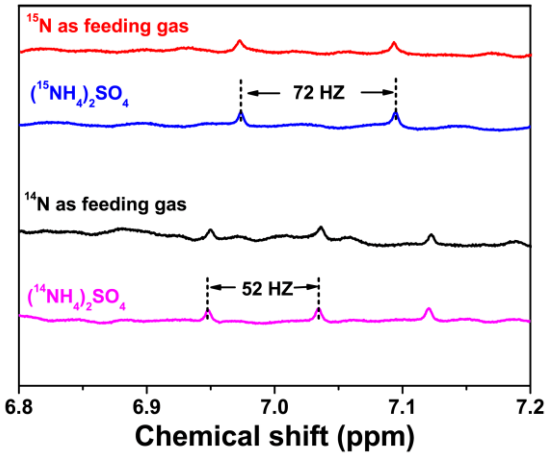

Fig. S8. ^{15}N isotope labelled experiment. ^{1}H NMR spectra of $(^{14}NH_4)_2SO_4$, $(^{15}NH_4)_2SO_4$ and the electrolyte fed by $^{14}N_2$ and $^{15}N_2$ after the electrolytic reaction.

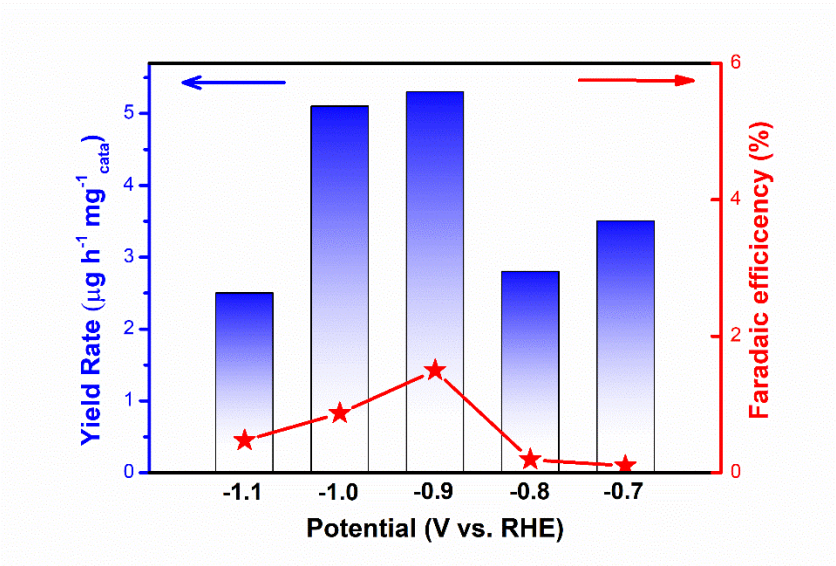

Fig. S9. Calculated NH_3 yield rate and Faradaic efficiency of 3R MoS_2-600/CP for the NRR at different potentials.

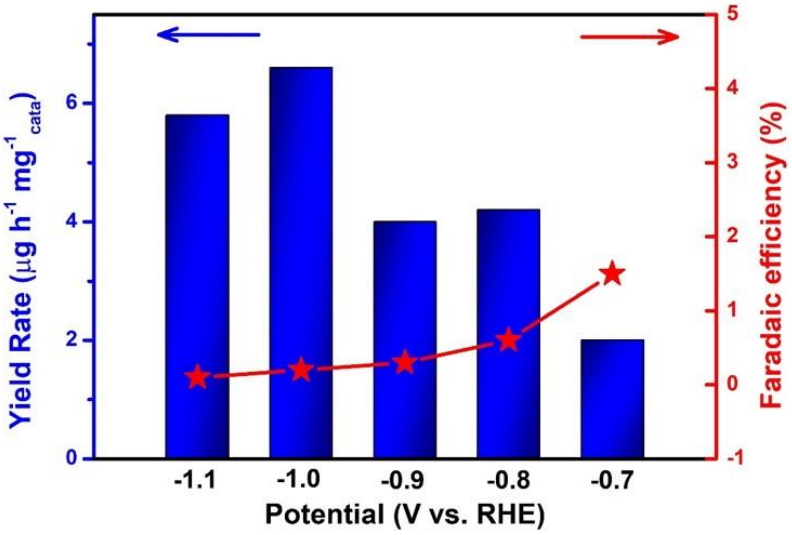

Fig. S10. Calculated NH_3 yield rate and Faradaic efficiency of 3R MoS_2-650/CP for the NRR at different potentials.

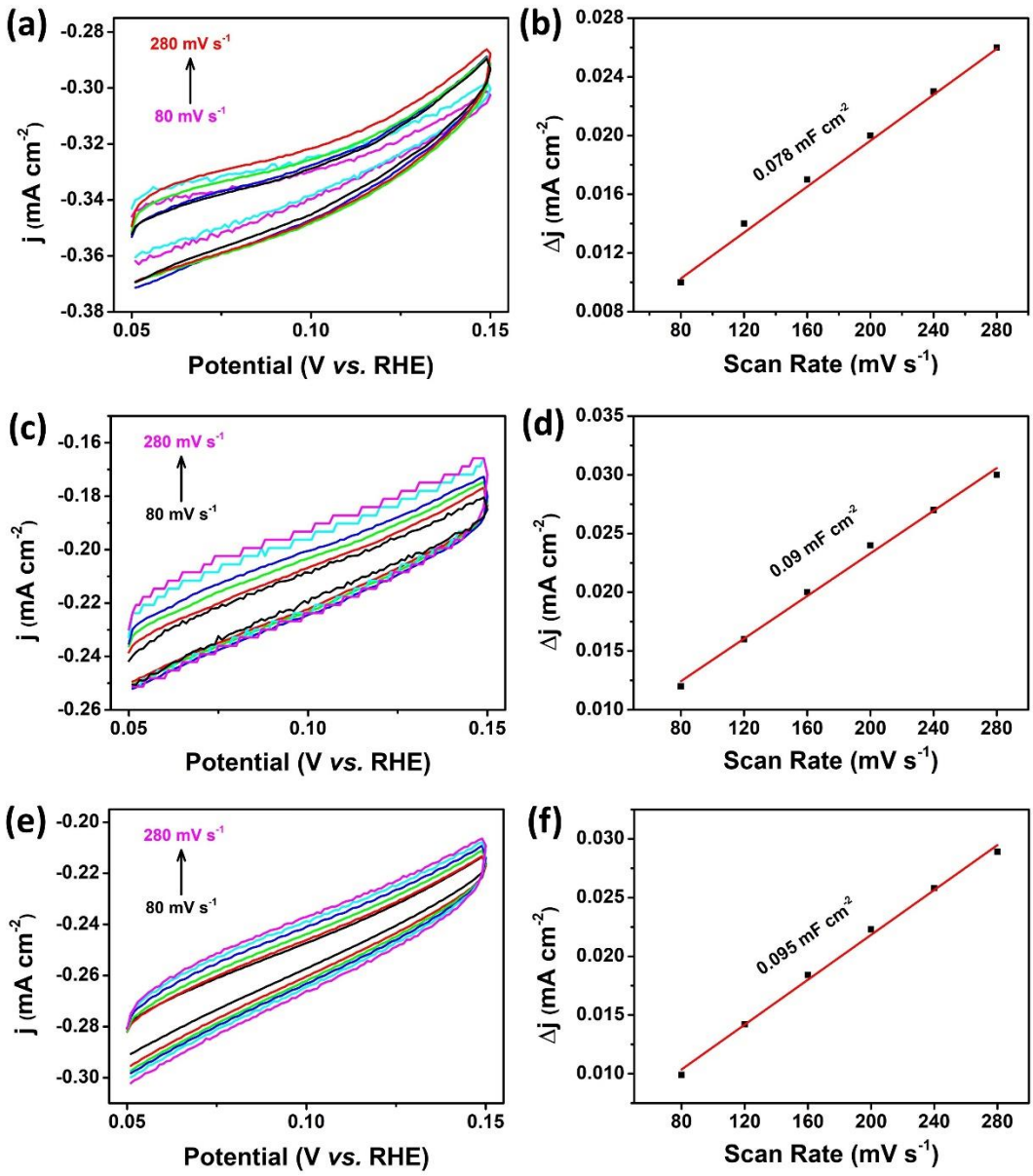

Fig. S11. CV curves of MoS_2-600 (a), MoS_2-650 (b) and MoS_2-700 (c) at 80-280 mV s^{-1} in the range of -0.05 and 0.15 V *vs.* RHE. Corresponding capacitive current densities at 0.1 V *vs.* RHE for MoS_2-600 (b), MoS_2-650 (d) and MoS_2-700 (f).

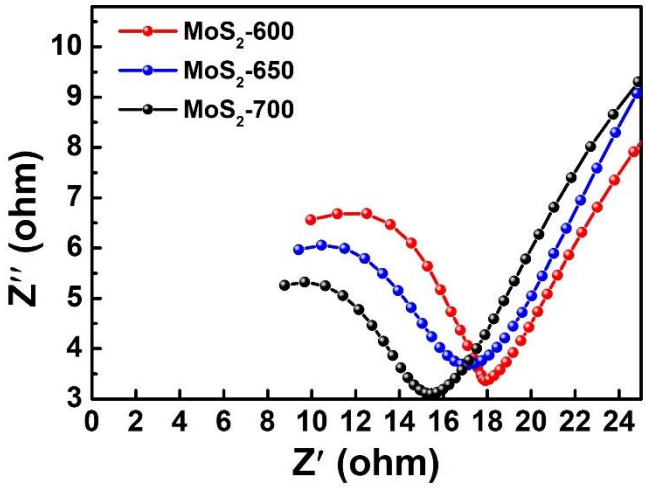

Fig. S12. Electrochemical impedance spectra of MoS_2-600/CP, MoS_2-650/CP and MoS_2-700/CP electrode measured at -1.0 V *vs.* RHE in Ar-saturated 0.1 M Na_2SO_4 electrolyte.

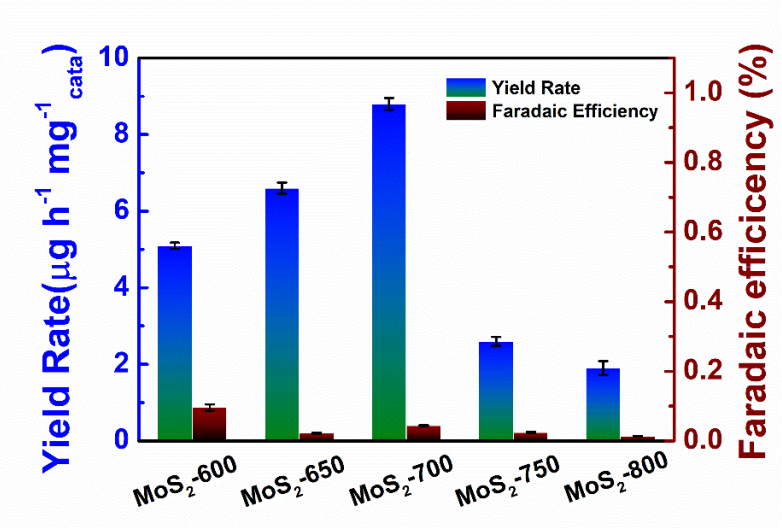

Fig. S13. Comparison diagram of calculated NH_3 yield rate and FE of MoS_2-600/CP, MoS_2-650/CP, MoS_2-700/CP, MoS_2-750/CP and MoS_2-800/CP for the NRR at -1.0 V *vs.* RHE.

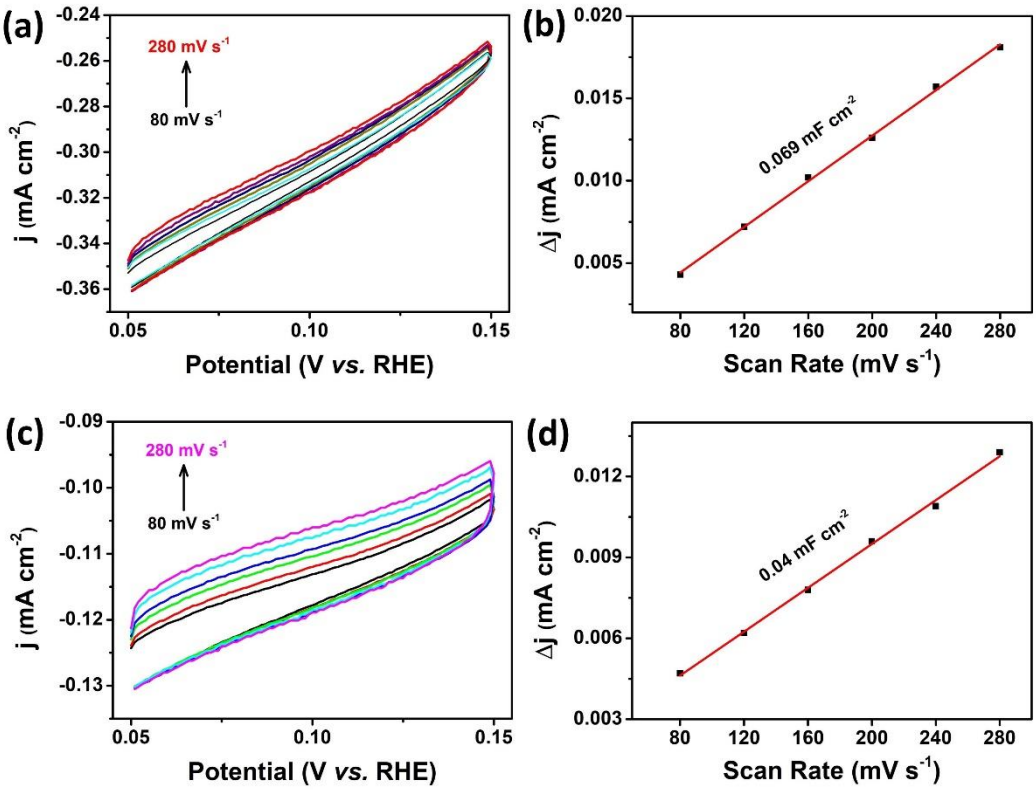

Fig. S14. CV curves of MoS_2-750 (a) and MoS_2-800 (c) at 80-280 mV s^{-1} in the range of -0.05 and 0.15 V *vs.* RHE. Corresponding capacitive current densities at 0.1 V *vs.* RHE for MoS_2-750 (b) and MoS_2-800 (d).

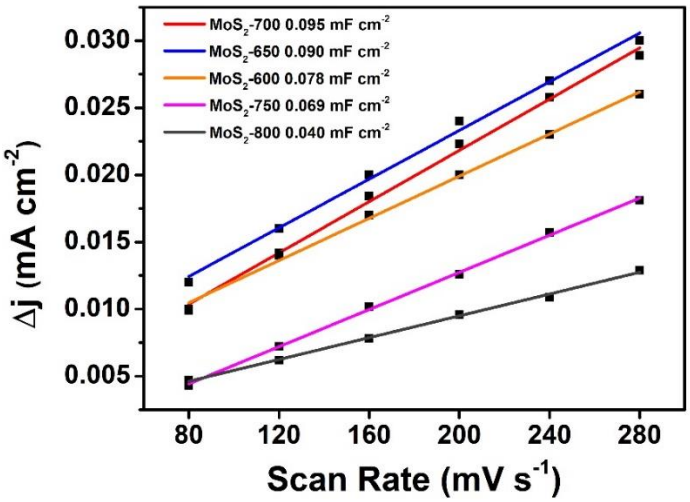

Fig. S15. Capacitive current densities at 0.1 V *vs.* RHE as a function of scan rates for MoS_2-600, MoS_2-650, MoS_2-700, MoS_2-750 and MoS_2-800.

References

[1] H. Cheng, L. Ding, G. Chen, L. Zhang, J. Xue, H. Wang, Molybdenum carbide nanodots enable efficient electrocatalytic nitrogen fixation under ambient conditions, *Adv. Mater*. 30 (2018) 1803694.

[2] L. Zhang, X. Ji, X. Ren, Y. Ma, X. Shi, Z. Tian, A.M. Asiri, L. Chen, B. Tang, X. Sun, Electrochemical ammonia synthesis via nitrogen reduction reaction on a MoS_2 catalyst: theoretical and experimental studies, *Adv. Mater.*, 30 (2018).

[3] B. H. R. Surrnto, D. Wang, L. M. Azofra, M. Harb, L. Cavallo, R. Jalili, D. R. G. Mitchell, M. Chatti and D. R. MacFarlane, MoS_2 Polymorphic Engineering Enhances Selectivity in the Electrochemical Reduction of Nitrogen to Ammonia, *ACS Energy Lett.*, 2019, 4, 430-435.

[4] H. Cheng, P. Cui, F. Wang, L.-X. Ding, H. Wang, High efficiency electrochemical nitrogen fixation achieved with a lower pressure reaction system by changing the chemical equilibrium, *Angew. Chem. Int. Ed.* 58 (2019) 15541–15547.

[5] Y. Zhou, X. Yu, X. Wang, C. Chen, S. Wang and J. Zhang, MoS_2 nanosheets supported gold nanoparticles for electrochemical nitrogen fixation at various pH value, *Electrochim. Acta*, 2019, 317, 34-41.

[6] X. Xu, B. Sun, Z. Liang, H. Cui and J. Tian, High-Performance Electrocatalytic Conversion of N_2 to NH_3 Using 1T-MoS_2 Anchored on Ti_3C_2 MXene under Ambient Conditions, *ACS Appl. Mater. Interfaces*,2020, 12, 26060-26067.